



## Experimental investigation of the fracture toughness of polycrystalline tungsten in the brittle and semi-brittle regime

Daniel Rupp\*, Sabine M. Weygand

Forschungszentrum Karlsruhe, Institute for Materials Research II, Hermann-von-Helmholtz-Platz 1, 76344 Eggenstein-Leopoldshafen, Germany

### A B S T R A C T

Tungsten is of special interest for the application as a plasma facing material in future fusion reactors. One drawback of tungsten as a structural material is that the brittle-to-ductile transition occurs at relatively high temperatures and thus tungsten is inherent brittle. In this work the fracture behavior and the fracture toughness of notched specimens are determined as a function of temperature in the brittle and semi-brittle regime. The influence of the microstructure of rolled polycrystalline tungsten on the fracture process is studied for different crack orientations relative to its texture. To gain insight in the responsible failure mechanisms the crack paths and the morphology of the fracture surfaces are characterized by means of scanning electron microscopy.

© 2009 Elsevier B.V. All rights reserved.

### 1. Introduction

Due to its low sputtering rate tungsten is usually considered as plasma facing material in current divertor designs [1] of future fusion reactors. Furthermore, tungsten is most suitable because of its thermophysical properties like high melting point or high thermal conductivity. A major drawback of tungsten as a structural material is its high brittleness at room temperature and its high ductile-to-brittle-transition temperature (DBTT). During operation, the divertor will be subjected to high thermal loads and high thermal gradients. The resulting thermal stresses could initiate cracks and thus lead to catastrophic failure.

So far, fracture mechanical studies of tungsten have been mostly restricted to single crystals [2] while fracture toughness data of polycrystalline tungsten are rare. The variation in the experimental data of recently published works [3,4] concerning the DBTT of polycrystalline tungsten and tungsten alloys exhibits again the strong influence of the production process. Particularly for brittle metals like tungsten, the microstructure plays a decisive role for the fracture behavior and the resulting fracture toughness. The aim of our experimental work is to gain a basic understanding of the failure mechanisms operating in polycrystalline tungsten which then enables us to identify possible ways of improvement.

### 2. Experimental procedure

#### 2.1. Material and microstructure

The material, which has been chosen for the experimental investigations, is rolled unalloyed 99.98% pure tungsten rods with a diameter of roughly 14 mm. This commercial material was produced by Plansee Metall GmbH, Reutte/Austria, in a powder metallurgical route. After sintering the rods experienced a break down rolling with a degree of deformation of 65% resulting in elongated grains with an aspect ratio of roughly 1:3 (see Fig. 1).

Additionally, the elongated grains possess a preferred orientation regarding the rolling direction, namely a fiber texture with the (110)-direction parallel to the rolling direction. However, the first investigations by means of Electron Back Scatter Diffraction (EBSD) showed that a distinct fiber texture exists only in the center of the rods. Thus only one specimen ( $3 \times 6 \times 27$  mm) was fabricated from the center of the rolled rods using Electrical Discharge Machining (EDM). To account for this anisotropic microstructure the specimens are extracted in three different directions (see Fig. 2): to promote fracture along the fiber axis (type Q2), to promote fracture perpendicular to the fiber axis and perpendicular to the elongated grains (type L), or perpendicular to the fiber axis but separating the grains (type Q1).

As the transverse specimens (Q1, Q2) are limited in their size, they needed to be brazed to two extension arms to obtain the desired geometry. The brazing process was carried out in high vacuum  $5 \times 10^{-5}$  mbar at a temperature of 1050 °C for half an hour using a Nickel based brazing alloy (STEMET 1311) [5]. The comparison of the optical micrographs of a sample in the initial and the annealed condition revealed no influence of the brazing process.

\* Corresponding author.

E-mail address: [daniel.rupp@imf.fzk.de](mailto:daniel.rupp@imf.fzk.de) (D. Rupp).

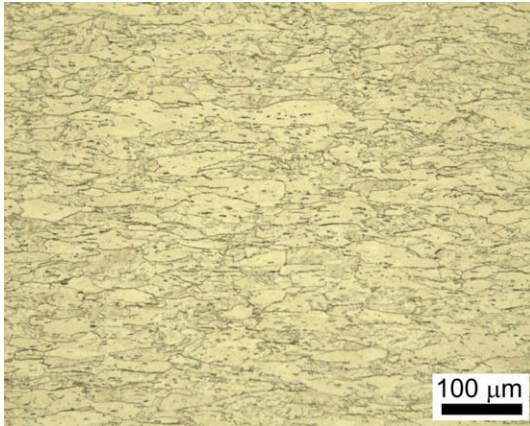


**Fig. 1.** Optical micrograph of a longitudinal section of a rolled tungsten rod. The micrograph shows elongated grains along the rolling direction with an aspect ratio of roughly 1:3.

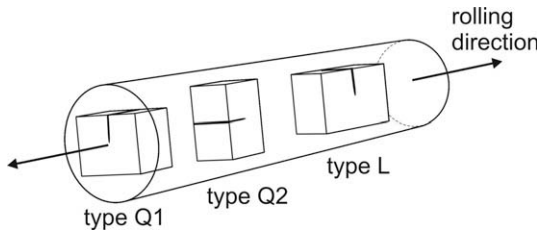


**Fig. 2.** Indication of the orientations of the investigated specimens: crack front parallel (Q1), crack front radial (Q2) and crack front tangential (L) to the rolling (fiber) direction.

Furthermore, no change in the Vickers hardness (429 HV30) could be observed.

## 2.2. Fracture mechanical testing

A servohydraulic testing machine (Schenck Hydropulse 63 kN) has been modified and combined with a climate chamber (Instron EC92) to perform 3-point-bending tests at different temperatures in the brittle to semi-brittle regime. The temperature of the specimen inside the chamber can be adjusted in a range from  $-150\text{ }^{\circ}\text{C}$  up to  $350\text{ }^{\circ}\text{C}$  by cooling with gaseous nitrogen and by a resistance heating, respectively. Additionally, the temperature was monitored with a resistance thermometer in the vicinity of the specimen during the measurement. The tests were performed in displacement control at a fixed transverse speed. For the experiments a transverse speed of approximately  $1\text{ }\mu\text{m/s}$  was chosen corresponding to a loading rate of  $0.5\text{ MPa m}^{1/2}/\text{s}$ . Force, displacement of the loading point and temperature were recorded with a data acquisition system at a sampling rate of 100 Hz during the bending test.

All tests presented here were conducted on notched specimens. Very sharp notches can be produced with a method using a razor blade as proposed by Nishida et al. [6] and successfully applied by Kübler [7] for fracture toughness tests of ceramics. Notches were produced by using the method mentioned above at the bottom of 3 mm deep notches fabricated by electric discharge machining (EDM), leading to a notch radius of roughly  $20\text{ }\mu\text{m}$  and an overall notch depth of about 3.2 mm.

## 3. Results

**Fig. 3** shows the determined fracture toughness as a function of the test temperature for all three different crack orientations.

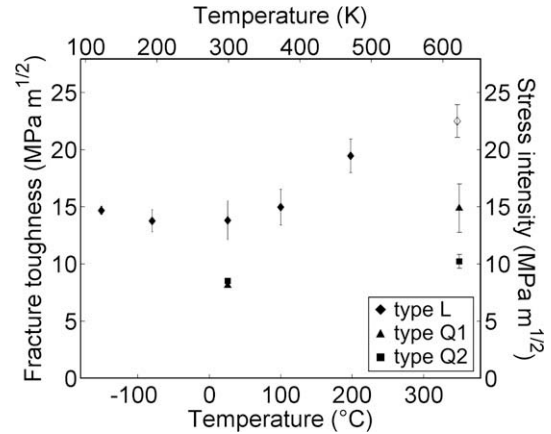


**Fig. 3.** Fracture toughness as a function of temperature for the three investigated crack orientations at a loading rate  $dK/dt$  of  $0.5\text{ MPa m}^{1/2}/\text{s}$ . The error bars mark the standard deviation of the measured values. The longitudinal specimens tested at  $350\text{ }^{\circ}\text{C}$  did not fail under Mode I. However, the stress intensity at crack initiation was calculated for comparability reasons and marked by the open symbol.

Three notched specimens were tested at each temperature, where all specimens failed macroscopically brittle. The fracture toughness has been calculated following the ASTM E399 [8] standard using the maximum applied stress when crack growth occurred and

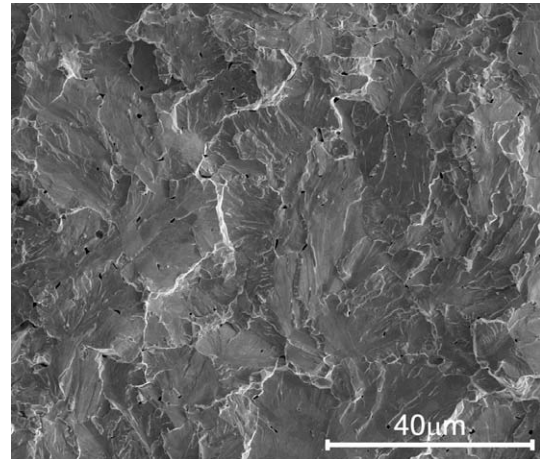


**Fig. 4.** Fracture surface of a longitudinal specimen (type L) tested at room temperature. The SEM image shows brittle fracture by pure cleavage. Some sintering pores can be observed at the grain boundaries.

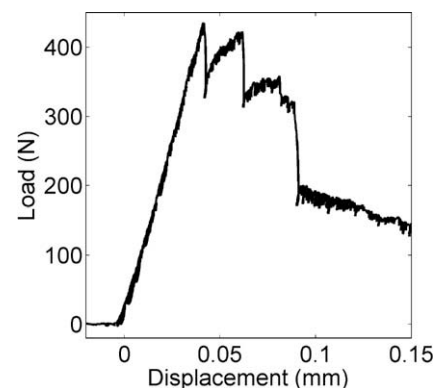


**Fig. 5.** Load-displacement record of a longitudinal specimen tested at  $200\text{ }^{\circ}\text{C}$  and a loading rate  $dK/dt$  of  $0.5\text{ MPa m}^{1/2}/\text{s}$ .

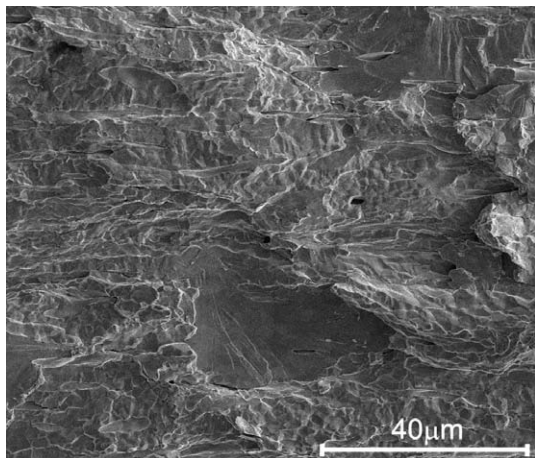


**Fig. 6.** Fracture surface of a transverse specimen (type Q1) tested at room temperature. The SEM shows a primarily intercrystalline fracture surface, but an amount of transcrystalline cleavage surfaces is also clearly visible.

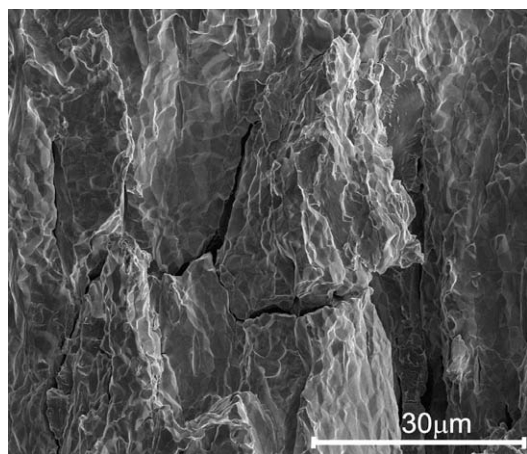


**Fig. 7.** Fracture surface of a transverse specimen (type Q2) tested at room temperature. The SEM image exhibits an intercrystalline fracture surface with only a small amount of cleavage surfaces compared to the fracture surface in Fig. 6.

the notch depth as crack length. As can be seen from Fig. 3 the fracture toughness of all three crack orientations raises with increasing temperature and the transverse specimens (type Q1, Q2) exhibit much lower fracture toughness than the longitudinal specimens (type L).

To gain insight in the responsible failure mechanisms the fracture surfaces of the tested specimens have been characterized by means of light and scanning electron microscopy (SEM). Special attention has been drawn to the longitudinal specimens, where a distinct change of the fracture behavior could be observed with increasing temperature. Whereas the specimens at room temperature and below failed catastrophically by pure transcrystalline cleavage (see Fig. 4), the load-displacement records of specimens at higher temperatures showed a perceptible pop-in at the crack initiation that was followed by a stepwise crack growth (see Fig. 5). At 350 °C the influence of the texture on the fracture process becomes particularly obvious; two symmetrical cracks could

be observed which proceeded macroscopically under approximately 70° with respect to the notch plane. Microscopically they propagated intercrystalline along the elongated grains and only a minor amount of transcrystalline cleavage could be observed. Despite the fact that the longitudinal specimen did not fail anymore under pure Mode I at 350 °C we calculated the stress intensity at crack initiation to be able to compare it with the fracture toughness scale.

Due to the microstructure, the transverse specimens showed a completely different behavior. The transverse specimens (type Q1, Q2) tested at room temperature and 350 °C exhibited a primarily intercrystalline fracture surface with an amount of transcrystalline cleavage surfaces (see Figs. 6 and 7). In contrast to the longitudinal specimens no change of the fracture behavior at elevated temperature could be observed for both transverse specimens and no crack deviation could be observed.

To address the issue of crack initiation in this textured tungsten in more detail, fracture tests will be performed on pre-cracked specimens in future studies and the results will be compared with the present results for notched specimens.

#### 4. Summary

The fracture toughness of polycrystalline tungsten has been investigated as a function of temperature and the crack orientation with respect to the rolling direction. The experimental results show the great influence of the microstructure on the fracture toughness and the failure mechanisms. With increasing temperature, the fracture toughness of all types of specimens increased in the investigated temperature range from –150 °C up to 350 °C. The longitudinal specimens showed higher fracture toughnesses than the transverse specimens. Whereas the transverse specimens failed by intercrystalline fracture at room temperature, the longitudinal specimens failed by pure transcrystalline cleavage. At elevated temperature a distinct change of the fracture behavior could be observed for the longitudinal specimens, whereas the fracture process gets dominated by intercrystalline failure.

#### Acknowledgments

The authors acknowledge the financial support from the German Science Foundation DFG under Grant No. SCHL1713/1 and the Research and Development Nuclear Fusion Programme of the Forschungszentrum Karlsruhe.

#### References

- [1] P. Norajitra, L.V. Boccaccini, A. Gervash, R. Giniyatulin, N. Holstein, T. Ihli, G. Janeschitz, W. Krauss, R. Kruessmann, V. Kuznetsov, A. Makhankov, I. Mazul, A. Moeslang, I. Ovchinnikov, M. Rieth, B. Zeep, J. Nucl. Mater. 367–370 (2007) 1416.
- [2] J. Riedle, Der Bruchwiderstand in Wolfram-Einkristallen: Einfluss der kristallographischen Orientierung, der Temperatur und der Lastrate, VDI-Verlag, 1995 (in German).
- [3] A. Giannattasio, S.G. Roberts, Phil. Mag. A 87 (2007) 2589.
- [4] M. Faleschini, H. Kreuzer, D. Kiener, R. Pippan, J. Nucl. Mater. 367–370 (2007) 800.
- [5] P. Norajitra, A. Gervash, R. Giniyatulin, T. Ihli, W. Krauss, R. Kruessmann, V. Kuznetsov, A. Makhankov, I. Mazul, I. Ovchinnikov, Fusion Eng. Des. 81 (2006) 341.
- [6] T. Nishida, G. Pezzotti, T. Mangialardi, A.E. Paolini, Fract. Mech. Ceram. 11 (1996) 107.
- [7] J. Kübler, Ceram. Eng. Sci. Proc. 18 (1997) 155.
- [8] ASTM E399-90 (1997), ASTM International, West Conshohocken PA, 2004.